Phase Transitions of Alkaline-Earth-Metal Disilicides $M_{AE}Si_2$ (M_{AE} = Ca, Sr, and Ba) at High Pressures and High Temperatures

Motoharu Imai*

National Institute for Materials Science, 1-2-1 Sengen, Tsukuba, Ibaraki 305-0047, Japan

Takumi Kikegawa

Photon Factory, National Laboratory for High Energy Physics, 1-1 Oho, Tsukuba, Ibaraki 305-0801, Japan

Received August 13, 2002. Revised Manuscript Received March 25, 2003

The structural phase transitions of alkaline-earth-metal disilicides $M_{AE}Si_2$ (M_{AE} = Ca, Sr, and Ba) at high pressures and high temperatures were investigated by the in situ X-ray diffraction technique. At pressures ranging from 0 to 15.5 GPa and temperatures ranging from 300 to 1300 K, $CaSi_2$ has three high-pressure phases: $EuGe_2$ phase, α-$ThSi_2$ phase, and AlB_2-like phase. At pressures ranging from 0 to 7.8 GPa and temperatures ranging from 300 to 1300 K, $SrSi_2$ has a high-pressure phase, the α-$ThSi_2$ one. $BaSi_2$ was confirmed to have three high-pressure phases, the $SrSi_2$, the $EuGe_2$, and $BaSi_2$-IV, in the pressure−temperature region ranging from 0 to 9.5 GPa and from 300 to 1300 K. In $M_{AE}Si_2$, the structures that appear at high pressures are the same as those of alkaline-earth disilicides or rare-earth disilicides with a smaller volume per chemical formula unit under ambient conditions. The observed structural sequence is different from that already known in other AX_2-type compounds. This is due to the fact that the same structure is observed at the same volume region in $M_{AE}Si_2$.

Introduction

The electrical properties and a pressure−temperature ($p-T$) diagram of $BaSi_2$ have been studied because (1) polymorphs are present, (2) each polymorph has a characteristic Si-atom configuration, and (3) the physical properties strongly depend on the structures of the polymorphs.[1−11] The study on the $p-T$ diagram revealed that the structural sequence of $BaSi_2$ is different from that known already in AX_2-type compounds.[6−8] $BaSi_2$ has four phases at pressures up to 7 GPa and temperatures from 300 to 1300 K, and the crystallographic form of the three phases is known. The stable phase at ambient conditions has the $BaSi_2$-type structure (space group *Pnma*, Figure 1a), and one of the high-pressure, high-temperature phases has the $SrSi_2$-type structure (space group $P4_332$, Figure 1b), while the other has the $EuGe_2$-type structure (space group $P\bar{3}m1$, Figure 1c).[1−5] In the $BaSi_2$-phase $BaSi_2$, Si atoms form tetrahedra,[1,2] and in the $SrSi_2$-phase $BaSi_2$, Si atoms form a three-dimensional network.[3] In the $EuGe_2$-phase $BaSi_2$, corrugated Si hexagonal layers alternate with hexagonal Ba layers along the [001] direction, and both layers stack in the AA sequence.[4] The structure of $SrSi_2$-phase $BaSi_2$ is the same as that of $SrSi_2$ at ambient conditions; the structure of $EuGe_2$-phase $BaSi_2$ is the same as that of $CaSi_2$ at ambient conditions[12] except for a small difference in the stacking sequence, which is described later. Thus, in $BaSi_2$, the structure that appears at high pressures is the same as that of the other alkaline-earth-metal disilicides with a smaller atomic-number metal. This observed structural sequence at high pressures is opposite the structural sequence known already in AX_2-type compounds, where A is a divalent or tetravalent cation and X is a halide or chalcogenide anion. In AX_2-type compounds, the structures that appear at high pressures are the same as those of other AX_2-type compounds with larger atomic-number cations in the same group.[13] Furthermore, in $M_{AE}Si_2$ (M_{AE} = Ba, Sr, and Ca), the same structure is observed in the same volume region: the volume of $SrSi_2$ at ambient conditions is in the volume region where the $SrSi_2$-phase

(1) Schäfer, H.; Janzon, K. H.; Weiss, A. *Angew. Chem., Int. Ed. Engl.* **1963**, *2*, 393.
(2) Janzon, K. H.; Schäfer, H.; Weiss A. *Z. Anorg. Allg. Chem.* **1970**, *372*, 87.
(3) Evers, J.; Oehlinger, G.; Weiss, A. *Angew. Chem., Int. Ed. Engl.* **1978**, *17*, 538.
(4) Evers, J.; Oehlinger, G.; Weiss, A. *Angew. Chem., Int. Ed. Engl.* **1977**, *16*, 659.
(5) Evers, J. *J. Solid State Chem.* **1980**, *32*, 77.
(6) Imai, M.; Hirano, T. In *Silicide Thin Films—Fabrication, Properties, and Applications*; Tung, R. T., Maex, K., Pellegrini, P. W., Allen, L. H., Eds.; MRS Symposia Proceedings No. 402; Materials Research Society: Pittsburgh, PA, 1996; p 567.
(7) Imai, M.; Hirano, T.; Kikegawa, T.; Shimomura, O. *Phys. Rev. B* **1997**, *55*, 132.
(8) Imai, M.; Hirano, T.; Kikegawa, T.; Shimomura, O. *Phys. Rev. B* **1998**, *58*, 11922.
(9) Evers, J. *J. Less-Common Met.* **1978**, *58*, 75.
(10) Imai, M.; Hirano, T. *J. Alloys Compd.* **1995**, *224*, 111.
(11) Imai, M.; Hirata, K.; Hirano, T. *Physica C* **1995**, *245*, 12.
(12) Böhm, J.; Hassel, O. *Z. Anorg. Allg. Chem.* **1927**, *160*, 152.
(13) Leger, J. M.; Haines, J. *Eur. J. Solid State Inorg. Chem.* **1997**, *34*, 785.

10.1021/cm0207954 CCC: $25.00
Published on Web 06/07/2003

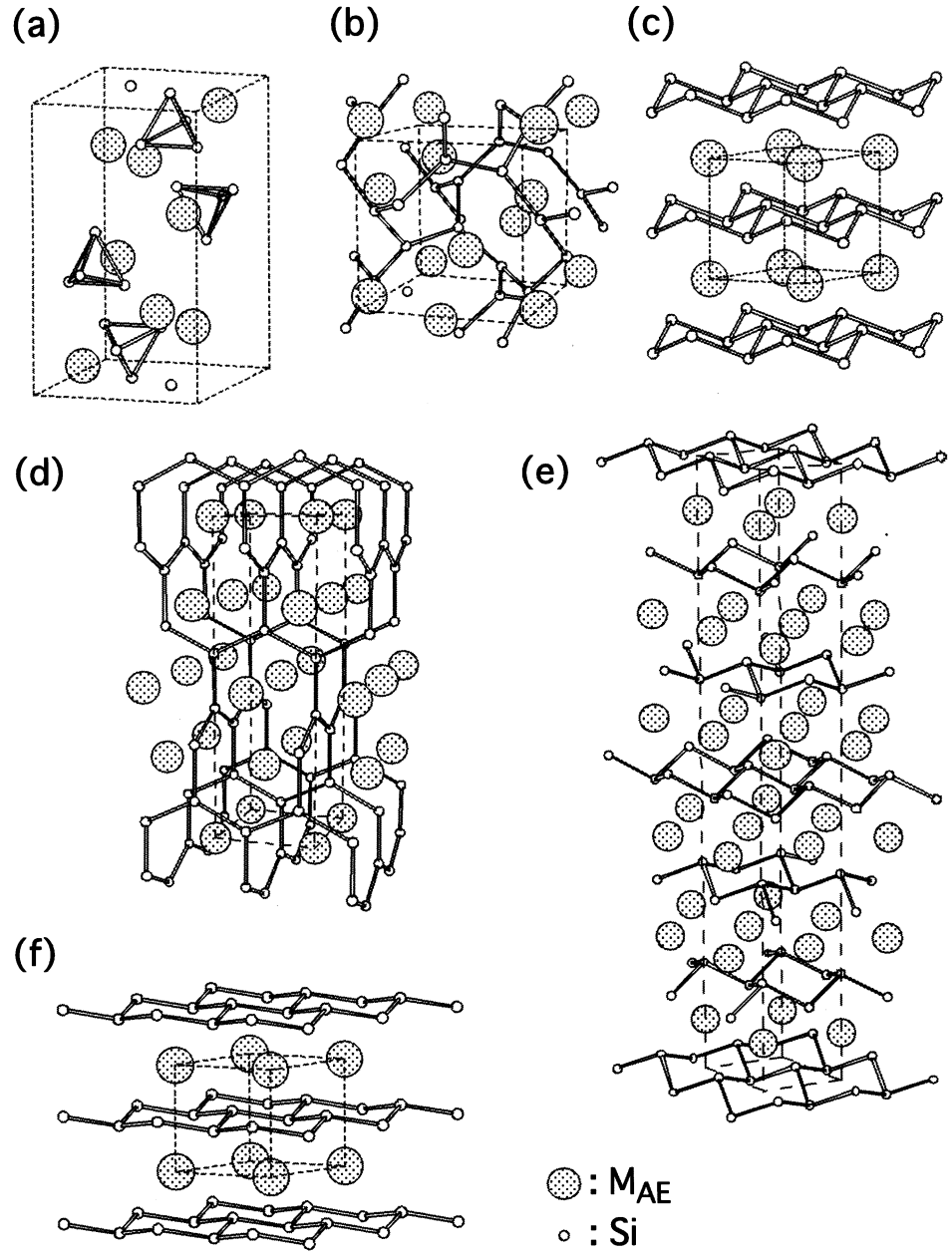

Figure 1. Crystal structures of $M_{AE}Si_2$: (a) the $BaSi_2$-type structure, (b) the $SrSi_2$-type structure, (c) the $EuGe_2$-type structure, (d) the α-$ThSi_2$ structure, (e) the $CaSi_2$-type structure, and (f) an AlB_2-like structure. $BaSi_2$ has the $BaSi_2$-type structure under ambient conditions, and the $SrSi_2$-type and $EuGe_2$-type ones at high pressures and high temperatures. $SrSi_2$ has the $SrSi_2$-type structures under ambient conditions and is deduced to have the α-$ThSi_2$ one at high pressures and high temperatures. $CaSi_2$ has the $CaSi_2$-type structure under ambient conditions, and the $EuGe_2$-type and an AlB_2-like ones at high pressures and room temperature. $CaSi_2$ is also deduced to have the α-$ThSi_2$ structure at high pressures and high temperatures.

$BaSi_2$ is observed, and that of $CaSi_2$ is in the region where only the $EuGe_2$-phase $BaSi_2$ is observed.[8] For a better understanding of the structural sequence and volume systematics observed in the $M_{AE}Si_2$, pressure experiments are necessary for the other alkaline-earth-metal disilicides, $SrSi_2$ and $CaSi_2$.

$SrSi_2$ has two crystallographic forms: the $SrSi_2$-type (Figure 1b) and the α-$ThSi_2$-type (space group $I4_1/amd$, Figure 1d),[2,14−18] as listed in Table 1. The $SrSi_2$ phase is stable at ambient conditions, and the α-$ThSi_2$ phase is metastable and synthesized by quench experiments. In the α-$ThSi_2$-phase $SrSi_2$, Si atoms form a three-dimensional network. There has been no report of in situ investigations of $SrSi_2$ at high pressures and high temperatures, although a pressure−temperature (p−T) diagram was constructed in a temperature range of 873−1473 K and a pressure range of 0−4 GPa with quenched samples.[17]

$CaSi_2$ has five crystallographic forms: four trigonal forms and a tetragonal one,[2,12,15,19−23] and the four related to this study are listed in Table 1. One trigonal

(14) Janzon, K. H.; Schäfer, H.; Weiss, A. *Angew. Chem., Int. Ed. Engl.* **1965**, *4*, 245.
(15) Evers, J.; Oehlinger, G.; Weiss, A. *J. Solid State Chem.* **1977**, *20*, 173.
(16) Evers, J. *J. Solid State Chem.* **1978**, *24*, 199.
(17) Evers, J. *J. Phys. Chem. Solids* **1979**, *40*, 951.
(18) Evers, J.; Oehlinger, G.; Weiss, A. *Z. Naturforsch.* **1983**, *38b*, 899.

Table 1. Structure Type of $SrSi_2$ and $CaSi_2$ Observed under Ambient Conditions and High-Pressure and High-Temperature Conditions

	ambient conditions	pressures from 1 to 4 GPa, high temperatures (quenching exp.)	pressures from 9 to 16 GPa, room temperature (in situ exp.)	pressures above 16 GPa, room temperature (in situ exp.)
$SrSi_2$	$SrSi_2$-type	α-$ThSi_2$-type		
$CaSi_2$	$CaSi_2$-type	α-$ThSi_2$-type	$EuGe_2$-type	AlB_2-like

$CaSi_2$ has the $CaSi_2$-type structure (space group $R\bar{3}m$) in which corrugated Si hexagonal layers alternate with hexagonal Ca layers along the [001] direction and both layers stack in the AABBCC sequence (Figure 1e).[2,12] This phase is stable at ambient conditions. The second trigonal $CaSi_2$, which is obtained by quick cooling of molten $CaSi_2$, has a structure in which corrugated Si hexagonal layers alternate with hexagonal Ca layers along the [001] direction and both layers stack in the ABC sequence (space group $R\bar{3}m$).[19,20] The third trigonal $CaSi_2$ has the $EuGe_2$-type structure.[22] This phase appears at high pressures ranging from 9 to 16 GPa and room temperature and can be quenched to ambient conditions. The structures of $CaSi_2$-phase $CaSi_2$ are the same as that of $EuGe_2$-phase $CaSi_2$ except for the difference in the stacking sequence. The last trigonal $CaSi_2$ has an "AlB_2-like" structure (space group $P\bar{3}m1$) in which slightly corrugated Si honeycomb layers alternate with Ca layers in the AA sequence (Figure 1f). In the AlB_2-type structure, Si layers are completely flat.[24] This phase was discovered by recent high-pressure experiments with a diamond anvil cell (DAC) and was reported not to be quenched to ambient conditions.[22] The tetragonal $CaSi_2$ has the α-$ThSi_2$-type structure,[15,23] which can be synthesized by quenching experiments.[15,22,23] Until now, phase transitions up to 4 GPa and 1373 K have been investigated by quenching experiments,[22] and those at room temperature up to 20 GPa have been investigated by in situ experiments with DAC.[22] However, the relationship among the four phases is still unclear, and the phase transitions at high temperatures and high pressures need to be studied in situ.

In this study, using the in situ X-ray diffraction technique, we investigate a $p-T$ diagram of $SrSi_2$ at pressures up to 7.8 GPa and temperatures up to 1300 K and that of $CaSi_2$ at pressures up to 15.5 GPa and temperatures up to 1300 K. We also investigate the phase transitions of $BaSi_2$ at about 9 GPa and temperatures up to 1219 K for comparison. It is found that the structures that appear at high pressures are the same as those of alkaline-earth disilicides or rare-earth disilicides with a smaller volume per chemical formula unit under ambient conditions in $M_{AE}Si_2$ and that the same structure is observed at the same volume region in $M_{AE}Si_2$.

Experimental Section

$BaSi_2$-phase $BaSi_2$ (nominal purity 98%), $SrSi_2$-phase $SrSi_2$ (nominal purity 98%), and $CaSi_2$-phase $CaSi_2$ (nominal purity 98%) were used as samples after arc-melting them to remove impurity phases.

High pressures were applied using the multi-anvil high-pressure apparatus MAX80, which is installed in the beam line of the TRISTAN accumulation ring (AR-NE5) at the National Laboratory for High Energy Physics.[25,26] Sintered diamond anvils with square flat-surface sizes of 6×6, 4×4, and 3×3 mm were used. We modified the sample assembly described in ref 26 for this study.[10] A powdered starting material was loaded in the h-BN capsule for the experiments at pressures below 11 GPa and in the MgO capsule for the experiments at pressures above 11 GPa. The capsule was set in the center of a boron-epoxy pressure-transmitting medium. The temperature was measured by an alumel−chromel thermocouple attached to the sample capsule. The pressure was evaluated from the lattice constant of an NaCl internal pressure marker.[27] The typical error of pressure was 0.1 GPa. X-ray diffraction patterns were measured by an energy-dispersive method using synchrotron radiation from the bending magnet. The measurements were performed at intervals of about 50−100 K with a heating rate of about 5 K/s. Lattice constants were obtained by the least-squares fitting of the indexed pattern.

The chemical compositions of several samples recovered after the pressure experiments were determined using electron probe microanalysis (EPMA) after the samples had been polished with an oil-based diamond slurry. It showed that there was no reaction between the capsule and sample nor any reduction.

Results

$CaSi_2$. Figure 2a shows the X-ray diffraction patterns of $CaSi_2$ for various pressures at room temperature. $CaSi_2$ undergoes the $CaSi_2$-to-$EuGe_2$ transition at 7.6 GPa, which is consistent with the transition pressure previously reported.[22] The transition is sluggish: the $CaSi_2$ phase still remains at 10.9 GPa, although a large part of the sample transforms into the $EuGe_2$ phase. At 14.8 GPa, a trace of the AlB_2-like phase was observed.

Figure 2b shows the X-ray diffraction patterns of $CaSi_2$ for various temperatures at about 5.7 GPa. $CaSi_2$ undergoes the $CaSi_2$-to-α-$ThSi_2$ transition at 783 K, accompanied with a 4.6% volume reduction. This transition is sharp compared with the $CaSi_2$-to-$EuGe_2$ transition. This result confirmed that the α-$ThSi_2$ phase is a high-pressure, high-temperature phase of $CaSi_2$ and that the α-$ThSi_2$ phase was quenched to ambient conditions, which is consistent with the fact that the α-$ThSi_2$ phase was synthesized by the quenching experiments.[22,23]

Figure 2c shows the X-ray diffraction patterns of $CaSi_2$ for various temperatures at about 10 GPa. At room temperature, the $EuGe_2$ phase is the main one, but a trace of the $CaSi_2$ phase still remains. When the sample is heated, it becomes almost a single $EuGe_2$

(19) Janzon, K. H.; Schäfer, H.; Weiss, A. *Z. Naturforsch.* **1968**, *23b*, 1544.
(20) Dick, S.; Öhlinger, G. *Z. Kristallogr. NCS* **1998**, *213*, 232.
(21) McWhan, D. B.; Compton, V. B.; Silverman, M. S.; Soulen, J. R. *J. Less-Common Met.* **1967**, *12*, 75.
(22) Bordet, P.; Affronte, M.; Sanfilippo, S.; Núñez-Regueiro, M.; Laborde, O.; Olcese,G. L.; Palenzona, A.; LeFloch, S.; Levy, D.; Hanfland, M. *Phys. Rev. B* **2000**, *62*, 11392.
(23) Evers, J. *J. Solid State Chem.* **1979**, *28*, 369.
(24) Hofmann, W.; Jäniche, W. *Z. Phys. Chem.* **1936**, *31B*, 214.
(25) Shimomura, O. *Physica B* **1986**, *139&140*, 292.
(26) Kikegawa, T.; Shimomura, O.; Iwasaki, H.; Sato, S.; Mikuni, A.; Iida, A.; Kamiya, N. *Rev. Sci. Instrum.* **1989**, *60*, 1527.
(27) Brown, J. M. *J. Appl. Phys.* **1999**, *86*, 5801.

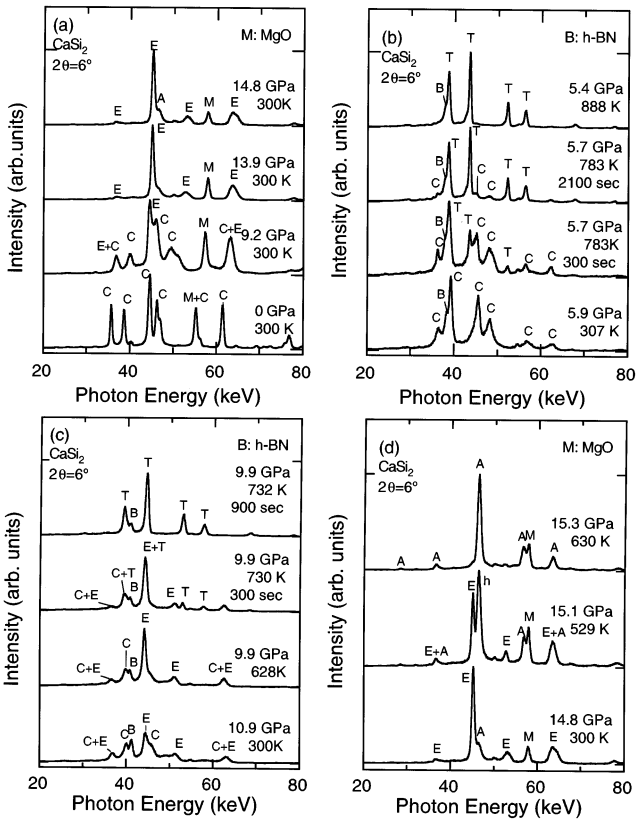

Figure 2. X-ray diffraction patterns of $CaSi_2$ for (a) various pressures at room temperature, (b) various temperatures at about 5.6 GPa, (c) various temperatures at about 10 GPa, and (d) various temperatures at about 14.8 GPa. The symbols "C," "T," "E," and "A" represent the reflections from the $CaSi_2$ phase, the α-$ThSi_2$ phase, the $EuGe_2$ phase, and the AlB_2-like phase, respectively. The symbols "M" and "B" show the reflections from the MgO and h-BN sample capsules, respectively.

phase at 581 K. When heated further, $CaSi_2$ undergoes the $EuGe_2$-to-α-$ThSi_2$ transition at 730 K, accompanied with a 2.2% volume reduction. This transition is sharp compared with the $CaSi_2$-to-$EuGe_2$ transition.

Figure 2d shows the X-ray diffraction patterns of $CaSi_2$ for various temperatures at about 15.2 GPa. At room temperature, the $EuGe_2$ phase is the main one, but a trace of the AlB_2-like phase exists. When the sample is heated, it becomes a single AlB_2-like phase at 630 K. When the transition occurs, the volume is reduced by 7.4%.

Figure 3 shows a $p-T$ diagram of $CaSi_2$. The broken lines are visual guides. The dotted line shows a reaction boundary for the $CaSi_2$-to-α-$ThSi_2$ transition determined by Evers.[23] In the $p-T$ region investigated, $CaSi_2$ has three high-pressure, high-temperature phases: the α-$ThSi_2$ phase, the $EuGe_2$ phase, and the AlB_2-like phase. The transition pressure for the $CaSi_2$-to-$EuGe_2$ transition (7.6 GPa) and that for the $EuGe_2$-to-AlB_2-like one (14.8 GPa) are consistent with that previously reported.[22] The observed reaction boundary for the $CaSi_2$-to-α-$ThSi_2$ transition is consistent with that determined previously for quenched samples.[23] The α-$ThSi_2$ phase is also a high-temperature phase of the $EuGe_2$ phase.

$SrSi_2$. When $SrSi_2$ is compressed up to 7.8 GPa at room temperature, the $SrSi_2$ phase has no phase transition; only the positions of the reflections shift to lower d-values, and the width of the reflections becomes broader. When the sample is heated at about 3.4 GPa, it shows no phase transition up to 1371 K.

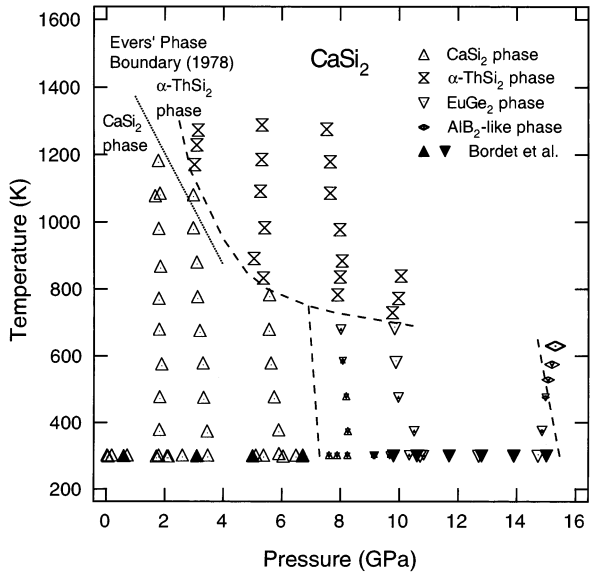

Figure 3. Pressure−temperature diagram of $CaSi_2$. At the $p-T$ conditions under which two phases are observed, the size ratio of the symbols is proportional to the intensity ratio of the strongest lines in the diffraction pattern. The dotted and broken lines show a reaction boundary determined by Evers (ref 23) and a visual guide, respectively.

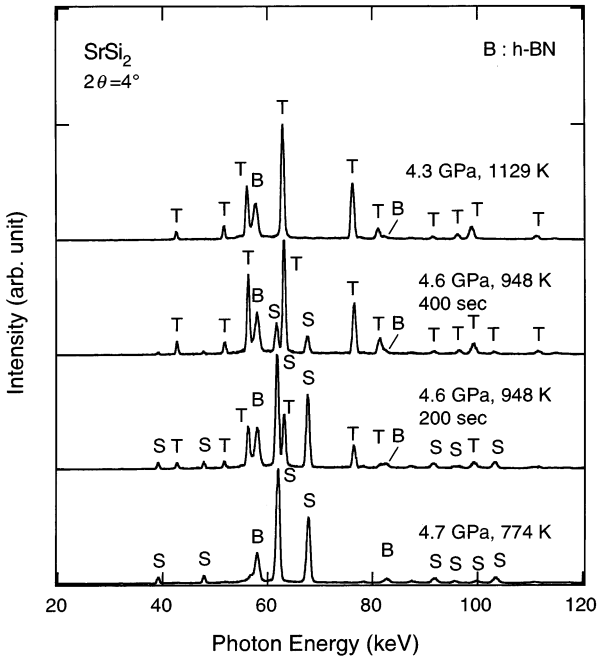

Figure 4. X-ray diffraction patterns of $SrSi_2$ for various temperatures at about 4.6 GPa. The symbols "S" and "T" represent the reflections from the $SrSi_2$ and α-$ThSi_2$ phases, respectively. The symbol "B" shows the reflections from the h-BN sample capsule.

Figure 4 shows the X-ray diffraction patterns of $SrSi_2$ for various temperatures at about 4.7 GPa. $SrSi_2$ undergoes the $SrSi_2$-to-α-$ThSi_2$ transition at 948 K. The transition is relatively sharp; a large part of the sample transforms in 800 s at 948 K. This transition was completed at 1083 K. The $SrSi_2$-to-α-$ThSi_2$ transition was also observed when the samples were heated at

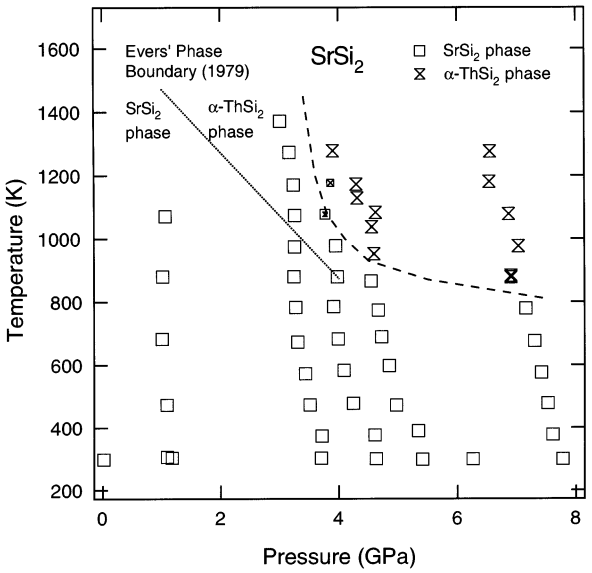

Figure 5. Pressure−temperature diagram of $SrSi_2$. At the $p-T$ conditions under which two phases are observed, the size ratio of the symbols is proportional to the intensity ratio of the strongest lines in the diffraction pattern. The dotted and broken lines show a reaction boundary determined by Evers (ref 17) and a visual guide, respectively.

about 4 and 7 GPa. At the transition for a given pressure, the volume decreased by a small amount (1.7% at 7.1 GPa).

Figure 5 shows a $p-T$ diagram of $SrSi_2$. The broken line shows a visual guide, and the dotted line is a reaction boundary for the $SrSi_2$-to-α-$ThSi_2$ transition previously determined for quenched samples.[17] In the $p-T$ region investigated, $SrSi_2$ has one high-pressure, high-temperature phase, the α-$ThSi_2$ one. The present diagram is consistent with that previously determined with quenched samples within the typical errors of pressure and temperature in the quenching experiments with the Belt-type apparatus.

$BaSi_2$. The $BaSi_2$ phase still remains at 9.5 GPa and room temperature. When the sample was heated at this pressure, $BaSi_2$ transformed from the $BaSi_2$ phase into the $EuGe_2$ one at 687 K. When the sample was heated further, the $EuGe_2$ phase transforms into $BaSi_2$-IV, as in the case of heating at 7.1 GPa.[8] Figure 6 shows a $p-T$ diagram of $BaSi_2$. The feature of the diagram is the same as that previously reported,[8] except for the maximum pressure. $BaSi_2$ has the following four phases in the $p-T$ region investigated: $BaSi_2$, $SrSi_2$, $EuGe_2$, and $BaSi_2$-IV.

Pressure Coefficients of the Lattice Parameters of Ambient-Phase $CaSi_2$, $SrSi_2$, and $BaSi_2$. Figures 7 and 8 show the lattice constants and volume of ambient-phase $CaSi_2$, $SrSi_2$, and $BaSi_2$ at room temperature as a function of the pressure, respectively. The lattice constants and the volume were normalized with values at ambient conditions. Table 2 lists the linear compressibility and a bulk modulus B_0. The bulk modulus was obtained by fitting the data to the Murnaghan equation with a B_0' of 4.[28] In the case of $CaSi_2$, the data at pressures at which only $CaSi_2$-phase $CaSi_2$ exists ($P < 8$ GPa) were used for fitting. The linear

(28) For example, Murnaghan, F. D. *Elastic Deformation of an Elastic Solid*; Dover: New York, 1967.

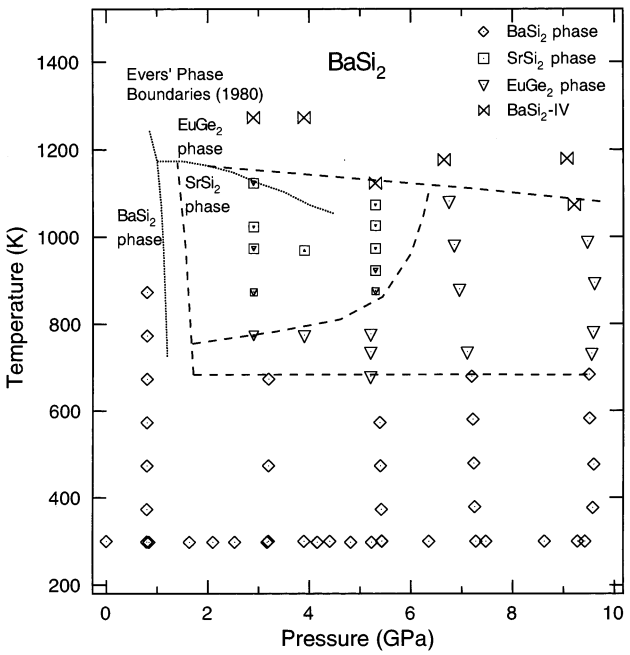

Figure 6. Pressure−temperature diagram of $BaSi_2$. At the $p-T$ conditions under which two phases are observed, the size ratio of the symbols is proportional to the intensity ratio of the strongest lines in the diffraction pattern. The dotted and broken lines show a reaction boundary determined by Evers (ref 5) and a visual guide, respectively.

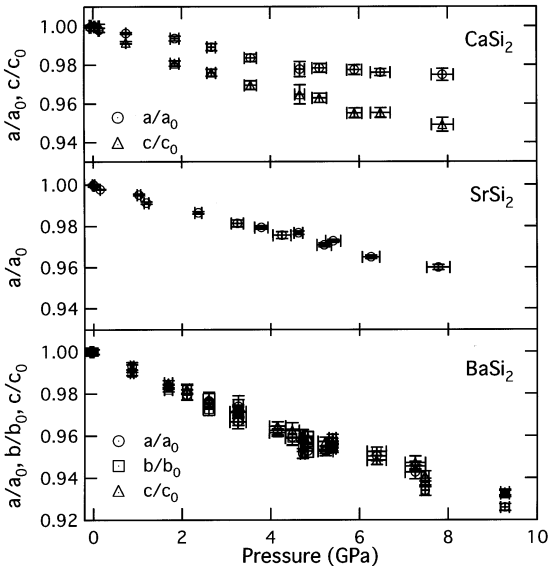

Figure 7. Lattice constants of $CaSi_2$-phase $CaSi_2$, $SrSi_2$-phase $SrSi_2$, and $BaSi_2$-phase $BaSi_2$ at room temperature as a function of the pressure. The lattice constants were normalized with values at ambient conditions.

compressibilities along three principal crystalline axes are about -8×10^{-3} GPa^{-1} for $BaSi_2$, indicating that the ambient-phase $BaSi_2$ is compressed isotropically. On the other hand, the compressibility along the *c*-axis direction ($-7.2(4) \times 10^{-3}$ GPa^{-1}) is twice as large as that along the *a*-axis direction ($-3.9(2) \times 10^{-3}$ GPa^{-1}) for $CaSi_2$, indicating that the ambient-phase $CaSi_2$ is compressed anisotropically. A comparison of B_0 among the three materials indicates that $BaSi_2$ is twice as compressible as $SrSi_2$ and $CaSi_2$ (27.9(4), 50.3(9), and 52.9(9) GPa for $BaSi_2$, $SrSi_2$, and $CaSi_2$, respectively). The bulk modulus of $BaSi_2$-phase $BaSi_2$ (27.9(4) GPa)

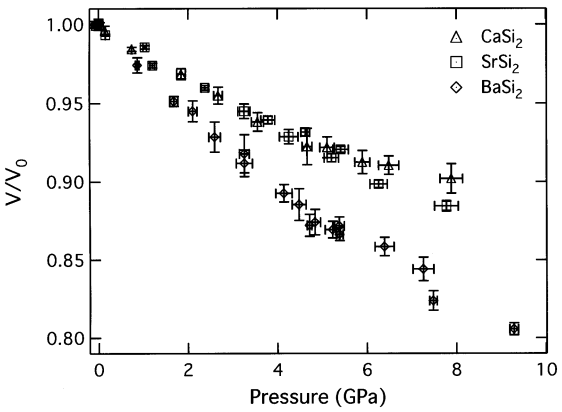

Figure 8. Volume per chemical formula unit of $CaSi_2$-phase $CaSi_2$, $SrSi_2$-phase $SrSi_2$, and $BaSi_2$-phase $BaSi_2$ at room temperature as a function of the pressure. The volume was normalized with values at ambient conditions.

Table 2. Pressure Coefficients of Lattice Constants and Bulk Moduli of $CaSi_2$-Phase $CaSi_2$, $SrSi_2$-Phase $SrSi_2$, and $BaSi_2$-Phase $BaSi_2$

	$d(a/a_0)/dP$ (10^{-3} GPa^{-1})	$d(b/b_0)/dP$ (10^{-3} GPa^{-1})	$d(c/c_0)/dP$ (10^{-3} GPa^{-1})	bulk modulus B_0 (GPa)
$CaSi_2$-phase $CaSi_2$	−3.9(2)		−7.2(4)	52.9(9)
$SrSi_2$-phase $SrSi_2$	−5.2(1)			50.3(9)
$BaSi_2$-phase $BaSi_2$	−8.2(3)	−7.7(3)	−7.6(2)	27.9(4)

is about half the calculated one (53 GPa).[29] This difference in B_0 between the experimental value and the calculated one is observed even when B_0' is treated as a variable parameter (B_0 = 31(1) GPa and B_0' = 2.5(5)).

Discussion

Structure Sequence of $M_{AE}Si_2$ at High Temperatures and High Pressures. $CaSi_2$ changes its structure from the $CaSi_2$-type to the $EuGe_2$-type and then to the AlB_2-like at high pressures and room temperature. At high pressures and high temperatures, $CaSi_2$ changes its structure from the $CaSi_2$-type or the $EuGe_2$-type into the α-$ThSi_2$-type. The structure that appears at high pressures cannot be related to the structure of other alkaline-earth-metal silicides with a smaller atomic number metal because neither the Mg−Si nor the Be−Si system forms a disilicide.[30] The α-$ThSi_2$-type structure is the structure that rare-earth metal disilicides $M_{RE}{}^{I}Si_2$ ($M_{RE}{}^{I}$= La, Ce, Pr, Nd, Sm, Eu, Gd, and Dy) have, and the AlB_2-type structure is the structure rare-earth metal disilicides $M_{RE}{}^{II}Si_2$ ($M_{RE}{}^{II}$ = Gd, Tb, Dy, Ho, Er, Tm, Yb, and Lu) have.[31] It is worth noting that (1) the number of valence electrons in rare-earth elements is two or three, which is the same as or close to that of alkaline-earth metals, that is, two, and (2) the volume per chemical formula unit of rare-earth-metal disilicides $M_{RE}Si_2$ (M_{RE} = $M_{RE}{}^{I}$ and $M_{RE}{}^{II}$) is smaller than that of $M_{AE}Si_2$.

$SrSi_2$ changes its structure from the $SrSi_2$-type to the α-$ThSi_2$-type at high pressures and high temperatures. The structure of the high-pressure, high-temperature phase is the same as that of $CaSi_2$. The structure sequence of $SrSi_2$ is close to that of $CaSi_2$, though $SrSi_2$ has neither the $CaSi_2$ nor the $EuGe_2$ phase as its high-pressure phase.

In the case of $BaSi_2$, the structure that appears at high pressures is the same as those of the other $M_{AE}Si_2$ with smaller atomic number metals, as shown in ref 8. It is worth noting that the volume of the $M_{AE}Si_2$ per chemical formula unit becomes smaller when the atomic number of the M_{AE} becomes smaller.

In summary, in $M_{AE}Si_2$, the structures that appear at high pressures are the same as those of disilicides with 10 or 11 valence electrons and smaller volume per chemical formula unit at ambient conditions.

Volume of $M_{AE}Si_2$ at High Temperatures and High Pressures. The previous work on $BaSi_2$[8] shows that the same structure is observed in the same volume region: the volume of $SrSi_2$-phase $SrSi_2$ is in the volume region where the $SrSi_2$-phase $BaSi_2$ is observed, and that of $CaSi_2$-phase $CaSi_2$ is in the region where only the $EuGe_2$-phase $BaSi_2$ is observed. In the case of $SrSi_2$ and $CaSi_2$, the α-$ThSi_2$-type and the AlB_2-like structures appear at high pressures and high temperatures. As described before, the α-$ThSi_2$-type and the AlB_2-type structures are observed in $M_{RE}Si_2$, and their volume per chemical formula unit is smaller than that of $M_{AE}Si_2$.[31] Therefore, it is interesting to compare the volume of $M_{AE}Si_2$ at high pressures and that of $M_{RE}Si_2$.

Figure 9 shows the volume per chemical formula unit of $M_{AE}Si_2$ as a function of the temperature. The solid triangles, squares, and circles represent the volume per formula unit of $CaSi_2$-phase $CaSi_2$,[8] $SrSi_2$-phase $SrSi_2$,[8] and α-$ThSi_2$-phase $LaSi_2$, respectively, at 0 GPa.[31] The α-$ThSi_2$-phase $LaSi_2$ has the largest volume among rare-earth metal disilicides with the α-$ThSi_2$-type structure, $M_{RE}{}^{I}Si_2$.[31] The broken line in Figure 9c shows the volume of $GdSi_{2-x}$, which has the largest volume among the rare-earth-metal disilicides with the AlB_2-type structure, $M_{RE}{}^{II}Si_2$.[31] In Figure 9a, the volume of $SrSi_2$-phase $SrSi_2$ at 0 GPa is in the volume region where the $SrSi_2$-phase $BaSi_2$ exists, and the volume of $CaSi_2$-phase $CaSi_2$ at 0 GPa is in the volume region where only the $EuGe_2$-phase $BaSi_2$ exists. In Figure 9b, the volume of α-$ThSi_2$-phase $LaSi_2$ at 0 GPa is in the volume region where the α-$ThSi_2$-phase $SrSi_2$ exists. In Figure 9c, the volume of α-$ThSi_2$-phase $LaSi_2$ at 0 GPa is slightly larger than the volume of α-$ThSi_2$-phase $CaSi_2$. However, the volume of $M_{RE}Si_2$ with the α-$ThSi_2$-type structure ranges from 54.33 to 63.41 Å^3,[31] and that of α-$ThSi_2$-phase $CaSi_2$ is in the same volume region. Thus, the same structure is observed in the same volume region in $M_{AE}Si_2$ at high temperatures above 750 K. On the other hand, at temperatures below 750 K, the ambient phase was quenched at high pressures in which high-pressure phases appear at higher temperatures.

The phase transitions at high pressures and temperatures above 750 K are accompanied by drastic Si-configuration changes. The resultant high-pressure, high-temperature phases are quenched to ambient

(29) Kitano, A.; Moriguchi, K.; Yonemura, M.; Munetoh, S.; Shintani, A.; Fukuoka, H.; Yamanaka, S.; Nishibori, E.; Takata, M.; Sakata, M. *Phys. Rev. B* **2001**, *64*, 045206.

(30) Massalski, T. B., Ed. *Binary Alloys Phase Diagram*, 2nd ed.; ASM International: Materials Park, OH, 1990.

(31) Maex, K., Rossum, M. V., Eds. *Properties of Metal Silicides*; INSPEC: Stevenage, 1995 and references therein.

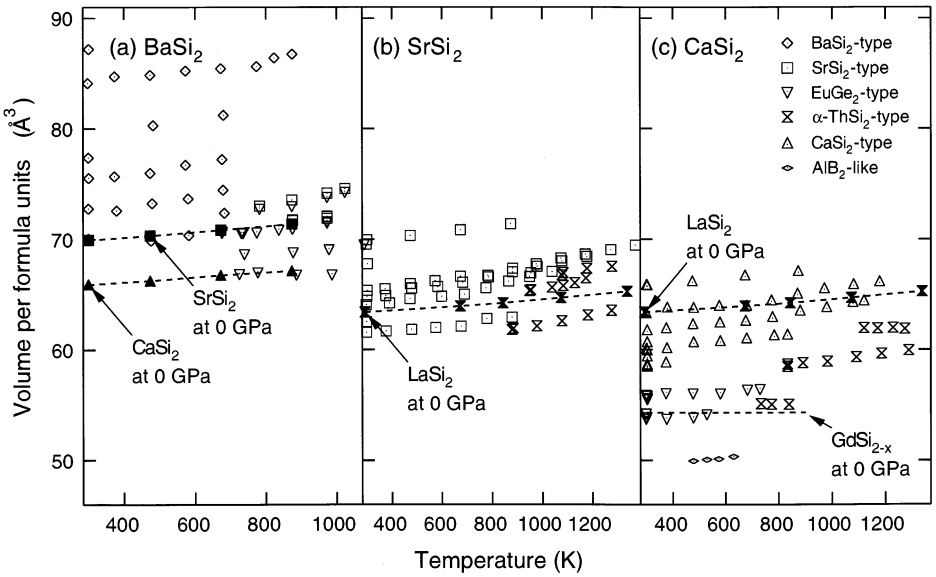

Figure 9. Volume per chemical formula unit of $M_{AE}Si_2$ at various pressure−temperature conditions: (a) $BaSi_2$, (b) $SrSi_2$, and (c) $CaSi_2$. The broken lines are used as a visual guide.

conditions. Furthermore, these quenched phases return to their starting phases when heated at ambient pressure, and the resultant starting phases remain unchanged after being cooled to room temperature at ambient pressure.[5,16,23] These facts suggest that the high-pressure, high-temperature phases are quenched as metastable phases and that the energy barriers for the transitions from high-pressure, high-temperature phases to the starting phases are large compared with thermal energy at room temperature. We think that the energy barrier for the transitions from the starting phase to the high-pressure, high-temperature phase is also large. When $M_{AE}Si_2$ is compressed at room temperature, the diffraction peak height becomes lower and the width becomes broader. When heated at high pressures, the height becomes higher and the width becomes narrower. This suggests that compression distorts the $M_{AE}Si_2$ inhomogeneously and that heating relaxes this inhomogeneous distortion, indicating that $M_{AE}Si_2$ needs a temperature higher than room temperature to relax the distortion. Therefore, $M_{AE}Si_2$ is expected to need a higher temperature to undergo phase transitions in which the atomic configuration changes more dramatically, suggesting that the energy barrier for the transition from the starting phase to the high-pressure, high-temperature phase is large. Thus, we think that pressure changes the stability of the phases and that temperature plays an important role to overcome the energy barrier for the transition in which the Si configuration changes drastically. Probably, this is the reason why $M_{AE}Si_2$ shows transitions accompanied by a drastic Si-configuration change when heated while the starting phase was quenched at room temperature in the pressure region in which the high-pressure phase appears at high temperature above 750 K. From the above, the kinetic effect on the phase transitions is assumed to be removed in the high-temperature region in Figure 9.

In the case of $BaSi_2$, the $SrSi_2$ phase appears at pressures ranging from 2 to 6.5 GPa, while it does not appear at pressures above 6.5 GPa. The volume of $SrSi_2$-phase $BaSi_2$ is about 1% larger than that of the $EuGe_2$-phase $BaSi_2$ under the same pressure−temperature conditions, suggesting that the $EuGe_2$ phase becomes more stable than the $SrSi_2$ phase in the smaller volume region. Since the volume of $BaSi_2$ decreases with increasing pressure, the volume of $BaSi_2$ is assumed to be too small to have the $SrSi_2$-type structure at pressures above 6.5 GPa. This is the reason why the $SrSi_2$ phase does not appear at pressures above 6.5 GPa.

Pressure Effect on the Structures of $M_{AE}Si_2$. The pressure effect on the structure of $CaSi_2$-phase $CaSi_2$ has been reported on the basis of the results of in situ experiments with DAC.[22] In the 0−7 GPa pressure range, $CaSi_2$-phase $CaSi_2$ is compressed anisotropically: the compressibility in the *c*−axis direction is twice as large as that in the *a*-axis direction, as can be seen in the present study. The interatomic distance and angles between Si atoms remain almost constant, and most of the *c*-axis compression can be attributed to the reduction of the separation between the Ca and Si layers, leading to a decrease in the average Ca−Si distance. This suggests that Ca atoms are more compressed than Si atoms. This is consistent with the bonding nature of $CaSi_2$-phase $CaSi_2$. $CaSi_2$-phase $CaSi_2$ has two-dimensional Si−Si layers, which are parallel to the *ab* plane direction, in which Si atoms are bonded covalently to each other.[32,33] The covalent bonds are expected to be harder than Ca atoms. Therefore, pressure squeezes the $CaSi_2$-phase $CaSi_2$ more along the *c*-axis than the *a*-axis direction.

Since we have no information on the internal parameters at high pressures in $BaSi_2$ and $SrSi_2$, we deduce the pressure effect on the structure in $BaSi_2$ and $SrSi_2$ by a comparison of the interatomic distance. Table 3 lists the interatomic distances and coordination numbers (CN) of the three polymorphs of $BaSi_2$,[34,3] the two of $SrSi_2$,[15,18] and the $CaSi_2$-phase $CaSi_2$ at atmospheric

(32) Fahy, S.; Hamann, D. R. *Phys. Rev. B* **1990**, *41*, 7587.
(33) Nishibori, E.; Saso, D.; Takata, M.; Sakata, M.; Imai, M. *Jpn. J. Appl. Phys. Suppl.* **1999**, *38-1*, 504.
(34) Daams, J. L. C.; Villars, P.; van Vucht, J. H. N. *Atlas of Crystal Structure Types for Intermetallic Phases*; ASM International: Materials Park, OH, 1991.

Table 3. Interatomic Distances and Coordination Numbers in Three Polymorphs of $BaSi_2$, Two of $SrSi_2$, $CaSi_2$, and $LaSi_2$

	nearest neighbor atoms of a metal atom	interatomic distance (Å)	nearest neighbor atoms of the Si atom	interatomic distance (Å)
$BaSi_2$-phase $BaSi_2$[a]	9 Si	3.341−3.645	3 Si	2.34−2.47
	or 11 Si	3.396−3.714		
$SrSi_2$-phase $BaSi_2$[b]	6 Si	3.37	3 Si	2.45
	2 Si	3.42		
$EuGe_2$-phase $BaSi_2$[b]	6 Si	3.28	3 Si	2.45
$SrSi_2$-phase $SrSi_2$[c]	6 Si	3.25	3 Si	2.39
	2 Si	3.47		
α-$ThSi_2$-phase $SrSi_2$[d]	4 Si	3.19	1 Si	2.33
	8 Si	3.34	2 Si	2.48
$CaSi_2$-phase $CaSi_2$[c]	6 Si	3.03	3 Si	2.45
	1 Si	3.06		
α-$ThSi_2$-phase $LaSi_2$[e]	4 Si	3.16	1 Si	2.33
	8 Si	3.24	2 Si	2.44

[a] Reference 34. [b] Reference 5. [c] Reference 17. [d] Reference 20. [e] Reference 35.

pressure[15] together with those of α-$ThSi_2$-phase $LaSi_2$ at atmospheric pressure.[35] In ref 8, Ba atoms are inferred to be compressed selectively in $BaSi_2$ at high pressures from the following arguments: (1) For the three polymorphs of $BaSi_2$, the interatomic distance between Ba and Si changes greatly compared with that between Si atoms. (2) A comparison among $BaSi_2$-phase $BaSi_2$, $SrSi_2$-phase $SrSi_2$, and $CaSi_2$-phase $CaSi_2$ shows the same tendency: the metal−Si distance changes significantly compared with the Si−Si distance. (3) Decreases in the interatomic distance by replacement of Ba with Sr and Ca are similar to the decreases made during the phase transitions of $BaSi_2$ at high pressures and high temperatures. (4) In the ambient phase $M_{AE}Si_2$, the decrease in the metal−Si distance seems to reflect the reduction in atomic volume of the alkaline-earth metal because the atomic volume of metal decreases in that order. And (5) therefore, the decrease in the Ba−Si distance observed in the polymorphs can be considered as the reduction of the atomic volume of Ba atoms by pressure.

This inference can also be applied to $SrSi_2$ because the change in the interatomic distances shows the same tendency as those of $BaSi_2$: the metal−Si distance changes much more than the Si−Si distance, as can be seen in the comparison between two polymorphs of $SrSi_2$ and between $SrSi_2$-phase $SrSi_2$ and α-$ThSi_2$-phase $LaSi_2$.

The discussion above suggests that, in $M_{AE}Si_2$, the M_{AE} atoms are compressed selectively at high pressures. Additionally, Figure 9 shows that the same structure appears at the same volume. We believe, therefore, that the reduction of the M_{AE} atom volume by pressure alters the interaction between atoms and causes a structural change when the M_{AE} atomic volume goes below a given volume.

Comparison with Other AX_2-Type Compounds. In the AX_2-type compounds, where A is a divalent or tetravalent cation and X a halide or chalcogenide anion, the structure that appears at high pressures is the same as those of the other AX_2-type compounds with larger atomic number cations in the same group.[13] In other words, the structure that appears at high pressures is the same as those of other AX_2-type compounds with the same number of valence electrons and a larger volume. This structural sequence in the AX_2-type compounds is opposite the observed structural sequence in $M_{AE}Si_2$.

The structural sequence of the AX_2-type compounds is discussed from the viewpoint of structural inorganic chemistry.[36] In the AX_2-type compounds, cation A is always surrounded by anions X, and the anions form polyhedra around the cation. These polyhedra are called coordination polyhedra. Under the condition that each X anion is in contact with the A cation, the CN of the A cation increases when the ratio of the ion radii r_A/r_X increases, where r_A and r_X are the ion radii of the A and the X ions, respectively. When the cations are replaced by larger atomic number cations in the same group, r_A increases and, consequently, the ratio r_A/r_X increases. Therefore, the compounds are expected to transform into a structure that consists of coordination polyhedra with higher CN. This explanation on the structural sequence observed by replacement of the cation is simple, but it is known to work well in the metal dioxides AO_2. Many dioxides crystallize with one of two simple structures, the larger A^{4+} ions being 8-coordinated in the fluorite structure and the smaller ions 6-coordinated in the rutile structure.

The general effect of the pressure is to increase the packing efficiency of the crystal structure. This is first achieved by compression and/or tilting of the coordination polyhedra and then by increasing the CN of the cation.[13] The reason that the high-pressure phase prefers a high CN can be discussed on the basis of the pressure dependence of the ratio r_A/r_X. When pressure is applied to the AX_2-type compounds, the anion X compresses more than the cation A because r_X is generally larger than r_A.[36] Consequently, the ratio r_A/r_X increases with the pressure. Therefore, the compound transforms into a structure that consists of coordination polyhedra with higher CN when pressure is applied. Thus, the pressure effect on the structure works in the same direction as that in which the replacement of cation by that with larger atomic number (larger atomic volume) affects the structure. What is important is that, in the AX_2-type compounds, the r_A/r_X determines the structure; r_A/r_X increases by both replacing the cation with that with a larger atomic volume and applying pressure, although the replacement changes r_A, and the pressure mainly changes r_X.

(35) Calculated using data in Nakano, H.; Yamanaka, S. *J. Solid State Chem.* **1994**, *108*, 260.

(36) Wells, A. F. *Structural Inorganic Chemistry*, 5th ed.; Clarendon Press: Oxford, 1984.

On the other hand, in $M_{AE}Si_2$, replacing the cation and applying pressure mainly affect the M_{AE} atom. Furthermore, the M_{AE} atomic volume is an important factor for the determination of the structure of $M_{AE}Si_2$. Therefore, the replacement of a cation with a larger volume cation works in the opposite direction in which applying pressure works because pressure mainly compresses the M_{AE} atoms. This is why the structural sequence of $M_{AE}Si_2$ at high pressures is opposite the structural sequence of the other AX_2-type compounds at high pressures.

Conclusion

The in situ X-ray diffraction technique revealed the structural sequence of $M_{AE}Si_2$ at high pressures and high temperatures. In $M_{AE}Si_2$, the structures that appear at high pressures are the same as those of disilicides with 10 or 11 valence electrons and a smaller volume per chemical formula unit at ambient conditions. The observed structural sequence is different from that known already in other AX_2-type compounds. We conclude that this is due to the fact that the same structure is observed at the same volume region in $M_{AE}Si_2$. Recently, new compounds, including M_{AE} and 14-group elements, such as clathrates, have been synthesized using quenching experiments. Therefore, a study on the structural sequence at high pressures would be very important for obtaining guidelines for the synthesis of new materials at high pressures and high temperatures.

Acknowledgment. The authors thank K. Tsuji of Keio University and K. Kusaba of Tohoku University for their useful advice with the experiments. The authors also thank Y. Uozu of the National Institute for Materials Science for machining jigs to make parts for high-pressure cell and T. Kimura and K. Nishida of the National Institute for Materials Science for the chemical composition determination using EPMA. This research was done under Grant 99G028 of the Photon Factory.

CM0207954